Experimental demonstrations in audible frequency range of band gap tunability and negative refraction in two-dimensional sonic crystal

Hélène Pichard,[a] Olivier Richoux, and Jean-Philippe Groby
Laboratoire d'Acoustique de l'Université du Maine, UMR-CNRS 6613, Avenue Olivier Messiaen, F-72085 Le Mans, Cedex 9, France

(Received 16 November 2011; revised 2 July 2012; accepted 16 July 2012)

The propagation of audible acoustic waves in two-dimensional square lattice tunable sonic crystals (SC) made of square cross-section infinitely rigid rods embedded in air is investigated experimentally. The band structure is calculated with the plane wave expansion (PWE) method and compared with experimental measurements carried out on a finite extend structure of 200 cm width, 70 cm depth and 15 cm height. The structure is made of square inclusions of 5 cm side with a periodicity of $L = 7.5$ cm placed inbetween two rigid plates. The existence of tunable complete band gaps in the audible frequency range is demonstrated experimentally by rotating the scatterers around their vertical axis. Negative refraction is then analyzed by use of the anisotropy of the equi-frequency surface (EFS) in the first band and of a finite difference time domain (FDTD) method. Experimental results finally show negative refraction in the audible frequency range. © *2012 Acoustical Society of America*. [http://dx.doi.org/10.1121/1.4744974]

PACS number(s): 43.25.Jh, 43.40.Fz, 43.20.El, 43.20.Ye [ANN] Pages: 2816–2822

I. INTRODUCTION

Phononic crystals are periodic composite material analogue of photonic crystals for light[1] characterized by the existence of band gaps where sound, vibration and elastic wave propagation are forbidden. In the literature, various structures made of two-dimensional phononic crystals were investigated: acoustic band gaps in square, triangular and rectangular lattices have been found for matrix-scatterer sonic crystal either both solids or fluids, or mixed solid-fluid. The first experimental observation of band gap has been made in a 2D periodic composite structure in the ultrasonic regime.[2]

In order to design sound barrier, it is important to demonstrate experimentally the properties of phononic crystal in the audible frequency range. In these frequencies, phononic crystals made of circular cross-section scatterer have been studied experimentally in the case of square[3,4] and triangular[3,5] lattices, the constituent being mixed solid-fluid or both solid. Also, sonic crystals made of resonant scatterers,[6–9] of porous coated cylinders,[10,11] or of elastic shells[12,13] have been designed to lead to wide range of attenuated frequencies.

Several theoretical studies pointed out that complete phononic band gap could be enlarged by rotating the scatterers.[14–16] Effectively, the lattice geometry (triangular, hexagonal, and square) and the scatterers shape, orientation and size, play an important role in the opening, enlargement or shifting of absolute acoustic band gaps.[17] By modifying one of these parameters, it is therefore possible to tune the band gaps of such arrangement. In this way, the present paper aims to study the acoustic propagation in two dimensional sonic crystal made of square shape scatterers. In order to demonstrate experimentally in the audible frequency range the tunability of a such system, the band diagram of the sonic crystal is studied experimentally and theoretically for different angles of rotation of the scatterers. A first experimental study of the sound attenuation by a sonic crystal made of square cross-section rods has been led[18] for a normal incidence and one angle of rotation of the scatterers in the high frequency regime of audible sound, which points out the pseudo band gap only on the ΓX direction. In the present paper, the acoustic attenuation of a square rods sonic crystal is investigated experimentally for two directions of the first Brillouin zone and for two rotation angles of the scatterers for frequencies in the speech intelligibility, i.e., between 1000 Hz and 3500 Hz. The tunability of a such system is demonstrated experimentally and, in the case of a non zero angle, the existence of a complete band gap is demonstrated.

Furthermore, phononic crystals exhibit other peculiar properties and in particular negative refraction of waves. In electromagnetism, the negative refraction was predicted by Veselago in 1968.[19] It has been observed in metamaterials[20,21] and photonic crystals[22] in the microwave and infrared frequency range, enabling, for example, the design of perfect lens, in which both propagating and evanescent waves contribute to the image reconstruction.[23] Such refraction[24] as well as superlensing effect[25] has also been observed with surface water waves in periodic structures of cylinders.

In acoustics, most of the works related to the negative refraction is dedicated to the focusing of ultrasonic waves.[26] Acoustic superlens have been designed[27] leading to high resolution ultrasonic imaging devices. Recently, experimental and numerical studies have also exhibited negative refraction for longitudinal and transversal elastic waves.[28–30] Identical phenomena have been observed for surface acoustic waves in the subgigahertz range.[31] Negative refraction of acoustic waves has mainly been studied numerically[32,33] and

[a]Author to whom correspondence should be addressed. Electronic mail: helene.pichard.etu@univ-lemans.fr

 0001-4966/2012/132(4)/2816/7/$30.00

observed experimentally[34,35] in the ultrasonic frequency range. Effectively, use of ultrasonic wave is the easiest way to study and observe these anomalous phenomena in spite of the large visco-thermal losses in phononic crystal for these frequencies,[36] because ultrasound generation can be highly directive. To our knowledge, the negative refraction in the audible frequency range has never been demonstrated. This paper proposes a preliminary experimental study of the refraction in sonic crystals for audible sound and demonstrates the existence of a negative refraction in the case of 2D square rods crystal.

To summarize, the propagation through a two-dimensional square lattice tunable crystal made of square cross-section scatterers is studied. A novel experimental set-up based on guided waves, presented in Sec. II, is used to demonstrate the tunability of this sonic crystal along two principal directions of the first Brillouin zone. To demonstrate this, experimental results obtained for two angles of rotation of the scatterers are compared in Sec. III. Finally, an analysis of the equi-frequency surface (EFS), confirmed by numerical results performed with finite difference time domain, allows to determine configuration parameters to exhibit experimentally negative refraction in the audible frequency range in Sec. IV.

II. EXPERIMENTAL SET-UP

A. The lattice sample

The 2D sonic crystal (SC) is shown in Fig. 1. Infinitely rigid square cross-section scatterers of dimensions $D \times D \times h = 5 \times 5 \times 15\,\text{cm}^3$ are distributed in air on a square lattice with periodicity $L = 7.5\,\text{cm}$. These scatterers are varnished wooden rods. The choice of this medium is motivated by the large impedance contrast between wood and the air

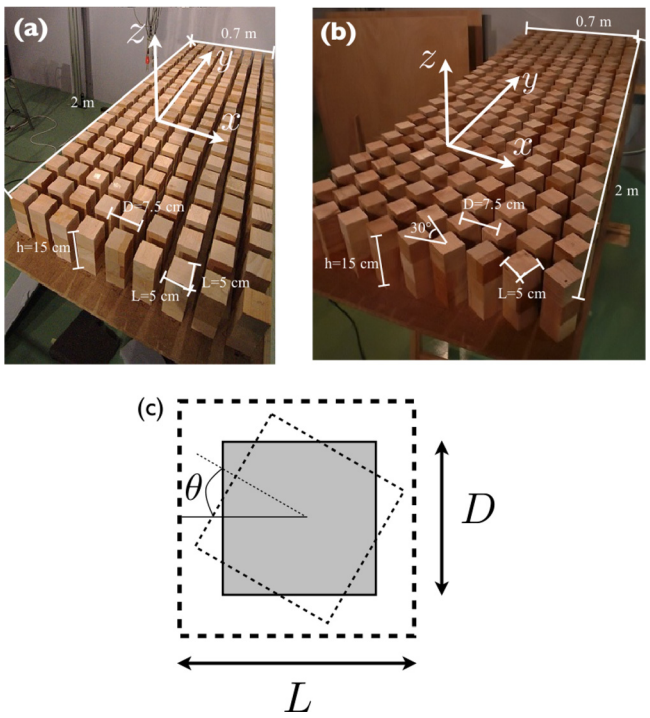

FIG. 1. (Color online) Experimental lattices, (a) $\theta = 0°$ and (b) $\theta = 30°$, and (c) unit cell.

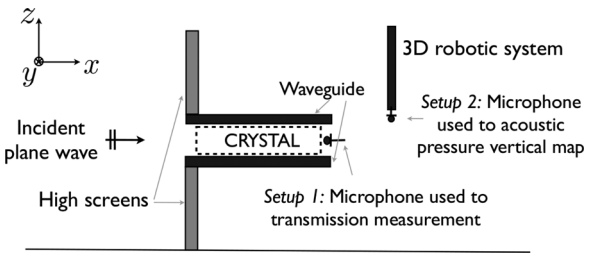

FIG. 2. Schematic representation of the experimental devices.

medium, which ensures that the scatterers can be considered as infinitely rigid ones. The crystal is $192.5 \times 65\,\text{cm}^2$ wide and is made of 234 scatterers arranged in 9 layers (in the propagating direction, i.e., along the x axis) of 26 scatterers (in the lateral direction, i.e., along the y axis), resulting in a filling fraction $ff = D^2/L^2 = 44\,\%$. Figure 2 presents a schematic view of the experimental device. The scatterers are placed inbetween two infinitely rigid wooden plates of $205 \times 70\,\text{cm}^2$ which formed a waveguide. The SC is centered between these two plates. The first cut-off frequency $f_c = c/(2h)$ of this waveguide is 1160 Hz. Above this frequency, higher modes can be excited. Nevertheless, the plane mode will mainly be excited because of the plane wave nature of the excitation used and described here after (Sec. II B). Therefore, the SC can be considered of infinite vertical extend and modeled in two dimensions. Direct sound propagation above and below the two plates of the waveguide could disturb the measurements behind the crystal. Two 100 cm high screens are then placed, on the source side, above and below these two plates in order to avoid such direct propagation. These two screens are perpendicular to the two plates, which form the waveguide, and are placed immediately at the entrance of the waveguide. This also enables to reduce diffraction of waves on the edges of the waveguide. The experiments are carried out in a semi-anechoic room. A cartesian coordinate system (x, y, z) is attached to the SC.

The scatterers can be rotated manually around their axis. This rotation is characterized by the angle θ between the scatterers sides and the lattice vectors [see Fig. 1(c)]. Figures 1(a) and 1(b) depict the two configurations studied in this article: the first configuration consists in 234 scatterers, whose sides are parallel to the lattice vectors, i.e., $\theta = 0°$, and the second configuration consists in the same 234 scatterers rotated around the vertical axis of $\theta = 30°$.

B. Sound source

In order to generate highly directive plane waves in the audible frequency range, an available parametric antenna[39] is used. This parametric antenna generates a powerful ultrasonic carrier wave at $f_0 = 40\,\text{kHz}$, which can be electronically modulated by an other wave at $f_0 - f_m$, with $f_m \in [200\,\text{Hz};\ 10\,\text{kHz}]$. Nonlinear self-demodulation processes, during the propagation of these two waves in the air, create an highly directive acoustic field beam at the modulation frequency f_m. The incident beam forms an angle α, measured counter-clockwise from the axis perpendicular of the crystal interface, i.e., the

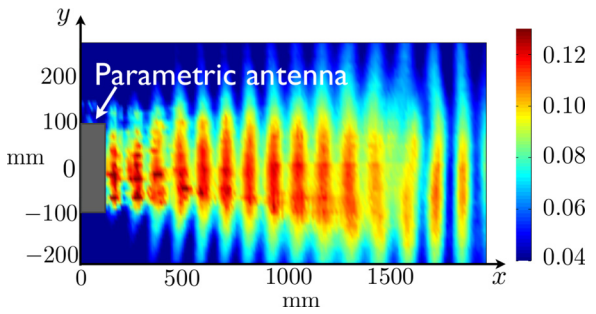

FIG. 3. (Color online) Amplitude pressure map performed in front of the parametric antenna in absence of the sonic crystal at 1600 Hz.

x axis. The parametric antenna is connected to the low frequency generator output of the spectrum analyzer (Stanford Research SR785).

It is usually accepted that the plane wave nature of the beam is established and that the maximum of pressure amplitude is reached after a propagation distance of $d_s = 120$ cm. This distance was validated by looking at an amplitude pressure horizontal map, presented in Fig. 3, performed in front of the parametric antenna in absence of the SC at 1600 Hz. The first interface of the crystal is then placed at this distance. The so-created beam is 35 cm wide and 50 cm height. The height of the acoustic beam being larger that the crystal height, i.e., the spacing between the two wooden plates, the field which is entering in the waveguide is a plane wave. This ensures that the plane mode of the guided wave is mainly excited. The lateral dimension of the crystal (192.5 cm) being larger than the width of the beam (35 cm), diffractions at the edge of the crystal are avoided.

C. Data acquisition system and post-processing

Two acquisition set-up were used and are presented in Fig. 2. In order to experimentally validate the band gap position and the band gap enlargement in function of θ, and therefore to prove the tunability of the system, the acoustic pressure is measured behind the crystal, i.e., transmission measurement, by means of a $1/2$ in. Bruel and Kjær microphone connected to a preamplifier and a conditioner. The microphone is placed at the end of the waveguide, i.e., between the two plates, at 2 cm behind the central scatterer (see set-up 1 in Fig. 2). The excitation signal is a chirp signal between 1000 Hz and 3500 Hz. The transfer function between the so-measured transmitted acoustic pressure and the signal generator is measured by use of the spectrum analyzer.

In order to point out the negative refraction, acoustic pressure (RMS value) vertical maps (in the $y-z$ plane) are measured by a $1/2$ in. Bruel and Kjær microphone piloted by a 3D robotic system, along the x axis behind the SC (see set-up 2 in Fig. 2). The spatial sampling is 1.2 cm along the y axis and z axis. The excitation is a sinus of frequency f. The acquisition of the acoustic pressure is performed using a sampling frequency $F_s = 10f$ (10 points per period $T = 1/f$) during a time length $T_a = N_s/F_s$ where $N_s = 1000$ (100 periods) is the samples number. The amplitude of the signal is determined by the RMS value of the acoustic pressure.

III. BAND STRUCTURE OF THE SONIC CRYSTAL

The band diagram can be efficiently determined by the plane wave expansion[40] (PWE) because of the high density contrast between the scatterers and the air medium. By use of theoretical models,[14,37,38] which take account for the scatterer rotation with respect to the lattice constant, the tunability effect in terms of width of the band gaps and also in terms of complete band gap appearance can be examined. These theoretical studies show that the width of the first band at normal incidence increases progressively when the rotation angle increases for a fixed filling fraction. To demonstrate this effect experimentally, two angles of rotation are chosen: $\theta = 0°$ and $\theta = 30°$. Figure 4 depicts the band diagrams of the SC calculated with the PWE for respectively $\theta = 0°$ and $\theta = 30°$ in the experimental configurations. While a band gap only exists along the ΓX direction for $\theta = 0°$, a complete band gap exists for $\theta = 30°$. For $\theta = 30°$, the arrangement of the scatterers induces more destructive interferences in the SC leading to a complete band gap.

The band diagrams calculated with the PWE method for these two specific angles θ are compared with transfer function measurements performed on the finite size crystal as described in Sec. II. Figure 5 depicts the band diagram calculated with the PWE along the ΓX direction between $[1000-3500]$ Hz for $\theta = 0°$ [Fig. 5(a)] and $\theta = 30°$ [Fig. 5(c)] as well as the corresponding experimental transfer function of the SC, respectively, for $\theta = 0°$ [Fig. 5(b)] and $\theta = 30°$ [Fig. 5(d)].

For $\theta = 0°$, two band gaps are noticed along the ΓX direction: the first between $[1500-2500]$ Hz and the second between $[3000-3500]$ Hz. These two gaps correspond to an amplitude loss of 15 dB in the measured transfer function. The measurements are in good agreement with the PWE predictions except for the second band gap: the experimental band gap is 50 to 100 Hz wider than the predicted one. This can be due to inherent disorder of the experimental handmade lattice.

For $\theta = 30°$, a band gap appears between $[1350-2900]$ Hz as pointed out by a decrease of 20 dB in the transfer function. This result is again in good agreement with the predicted one and shows an increase of the first band gap width when compared to the previous case with $\theta = 0°$. According to the

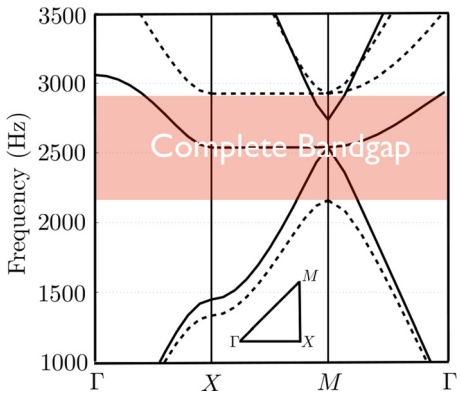

FIG. 4. (Color online) Band diagrams calculated with the PWE method, as shown in Refs. 14 and 37 when the lattice periodicity is $L = 7.5$ cm ($ff = 44$ %) for $\theta = 0°$ (continuous line) and $\theta = 30°$ (dotted line). The colored region illustrates the complete band gap for $\theta = 30°$.

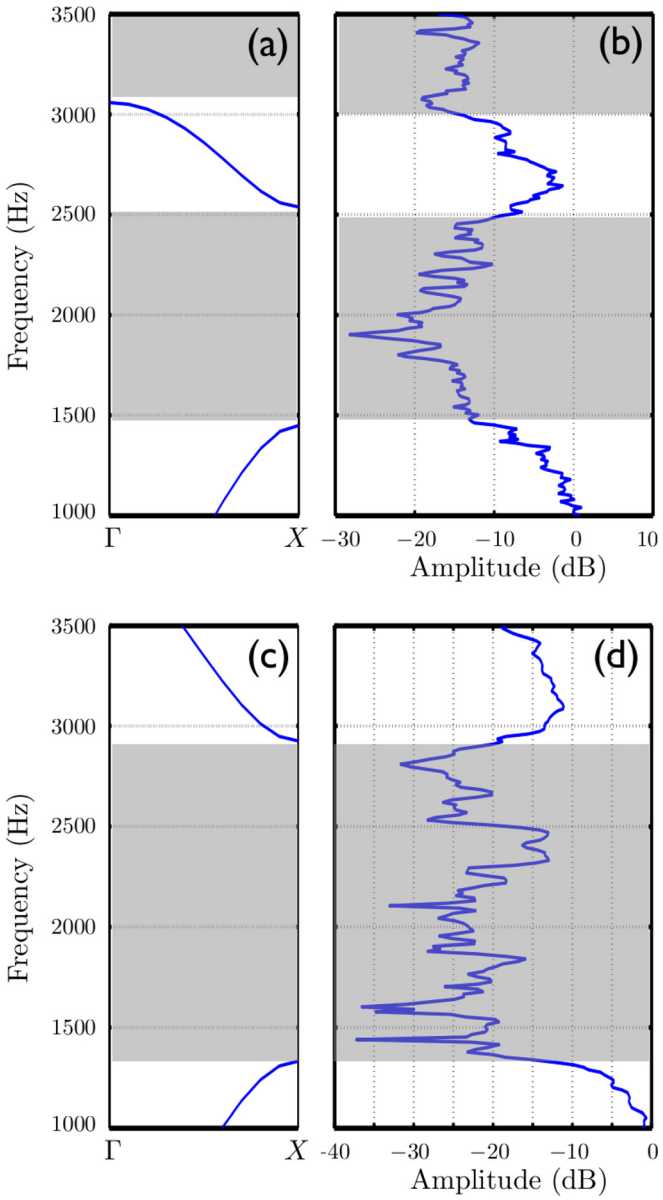

FIG. 5. (Color online) Band diagrams calculated by PWE along the ΓX direction for (a) $\theta = 0°$ and (c) $\theta = 30°$. Transfer function of the SC for a normal incidence for (b) $\theta = 0°$ and (d) $\theta = 30°$. The gray regions illustrate the band gaps.

PWE, a complete band gap can be obtained with the $\theta = 30°$ crystal. In order to validate the completeness of the band gap, the same experiment is carried out with $\alpha = 45°$, which enables to experimentally investigate the $M\Gamma$ direction.

Figure 6 depicts the PWE prediction [Fig. 6(a)] and the experimental transfer function [Fig. 6(b)] along the $M\Gamma$ direction for the $\theta = 30°$ crystal. A band gap, pointed out by a decrease of 15 dB in the measured transfer function, is noticed experimentally between $[1900-2900]$ Hz, which qualitatively corresponds to the PWE prediction. Nevertheless, this experimental band gap is wider than the predicted one. This can be explained by the refraction angle between the air medium and the crystal, which is frequency dependent and make the angle of the excitation wave inside the crystal slightly different. This can also be explained by the inherent disorder of the arrangement, the finite dimensions

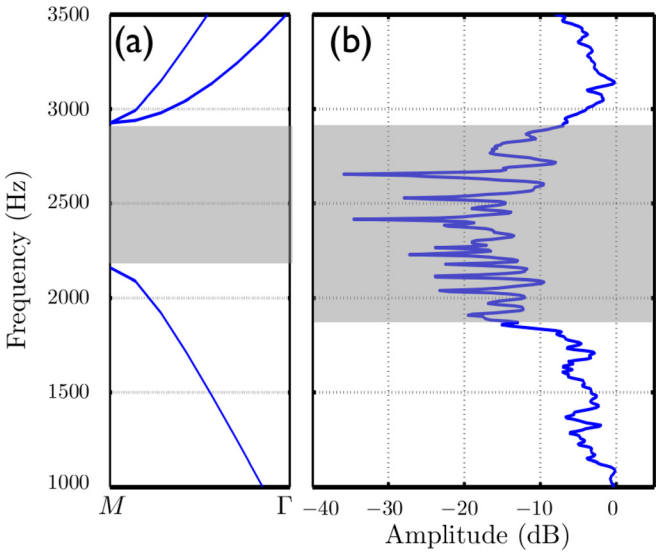

FIG. 6. (Color online) (a) Band diagrams calculated by PWE along the $M\Gamma$ direction with $\theta = 30°$. (b) Amplitude transfer function of the SC with $\theta = 30°$ with oblique incidence corresponding to the $M\Gamma$ direction. The gray region illustrates the band gap.

of the experimental SC which can enlarge the band gap width, and to a shift of the angle of incidence. Effectively, a small variation in the angle of incidence can lead to important discrepancies between the experimental and the theoretical results for non normal incidence. The oscillations that are noticed in the band gap are due to the fact that the transfer functions are calculated by measuring the field in a point close to the crystal. Effectively, when the microphone is close enough to the SC, constructive interferences that are normally trapped in the crystal can be recorded.

These experimental results, obtained in two configurations ($\theta = 0°$ and $\theta = 30°$), highlight the fact that the width of the band gaps is sensitive to the rotation angle of the scatterers. The apparition of a complete band gap along the ΓX and ΓM directions in the transmission and the tunability of this type of crystal are demonstrated experimentally for the first time in the speech intelligibility frequency range. This offers the opportunity to design numerous applications for audible sound problem.

IV. EXPERIMENTAL STUDY OF THE NEGATIVE REFRACTION

In order to study and visualize acoustic wave refraction in the considered sonic crystal, the equifrequency surface (EFS) of the band structure is analyzed. The PWE method is used to construct the EFS contours.[41] The EFS are constructed for the acoustic waves propagating from air to the SC along the ΓX direction (in the $\mathbf{k}$-space) for $\theta = 0°$. Figures 7(a) and 7(b) represent, respectively, a scheme of the refraction process inside the finite size crystal and the EFS in the SC at $f = 2300$ Hz and for K_x and K_y ranging from 0 to 1 (in units of π/a). The perfect circle is the air contour, namely $\omega = c\|\mathbf{k}_{air}\|$, while the convex contour around the point M of the Brillouin zone is the one of the crystal. In this case, negative refraction is observed for an angle of incidence of $\alpha = 25°$. Indeed, the plots of the incident wave

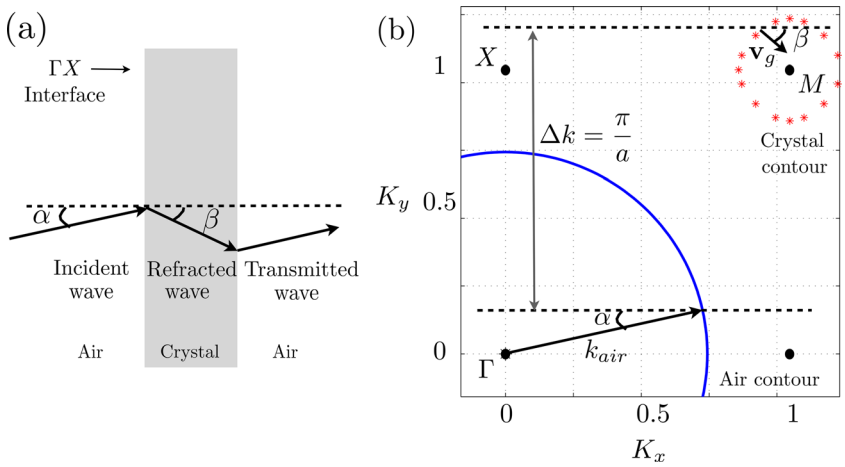

FIG. 7. (Color online) (a) Schematic of negative refraction process and (b) EFS in the **k** space of the air and SC at $f = 2300$ Hz. $\mathbf{k_{air}}$ and $\mathbf{v}_g$ are the wave vector in the air and the group velocity in the SC, respectively. With a vertical conservation of frequency shifted Δk, an incident plane wave with $\mathbf{k_{air}}$ will be refracted negatively.

vector in the air and of the conservation of frequency (dashed lines in Fig. 7) allow to geometrically determine the direction of the refracted wave inside the crystal. Because of the periodicity $\Delta k = \pi/a$ of the SC, the dashed line can be shifted at corresponding points within the entire K space.[35] The point where this dashed line intersects the crystal contour determines the direction of the group velocity $\mathbf{v}_g$, which is toward the point M. The group velocity (and hence the direction of energy propagation) of sound waves inside the crystal is given by the gradient of the angular frequency with respect to the wave vector, i.e., $\mathbf{v}_g = \nabla\omega(\mathbf{k})$, and is always perpendicular to the equifrequency contours. The angle of refraction β is the one between the conservation of frequency and $\mathbf{v}_g$. In this case, a wave impinging the crystal with an incident angle $\alpha = 25°$ is refracted in the crystal with an angle β of approximately $-30°$. These calculations are confirmed by numerical simulations performed with a finite difference time domain (FDTD) code coupled with the PML method.[42] A Gaussian beam located on the left side of the SC radiates a mono-frequency wave at $f = 2300$ Hz. The SC is made of 6 layers of 20 scatterers width and the filling fraction is $ff = 44\%$. Figure 8 shows the calculated pressure field when the angle of incidence is $\alpha = 25°$. The refraction angle is consistent with the one estimated from the EFS analysis and simulation result clearly demonstrates the existence of negative refraction in the audible frequency range. The negative refraction in the audible frequency range is now investigated experimentally. The incident beam is adjusted in order to impinge the SC with an angle of incidence of $\alpha = 25°$ in its central region, Fig. 9(a). Figure 9(b) depicts vertical transmitted pressure field maps (in the $y - z$ plane) for $z \in [-0.1 \ : \ 0.1]$ and $y \in [-0.5 \ : \ 0.5]$ measured behind the crystal along the x axis for $d = [0.1, 0.2, 0.3, 0.4, 0.5]$ m. These vertical pressure maps point out the existence of a

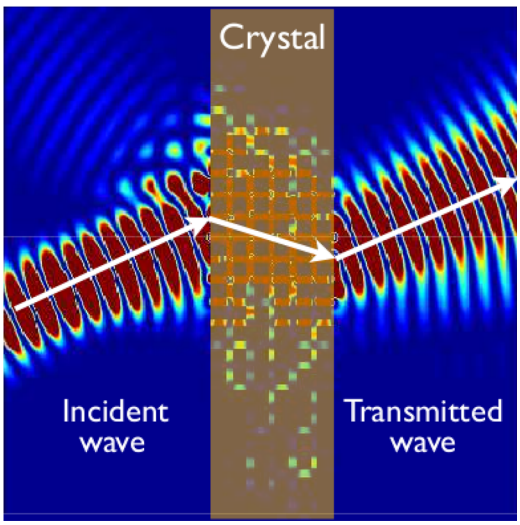

FIG. 8. (Color online) FDTD simulation of refraction in a square rod sonic crystal for $f = 2300$ Hz and with an incident angle $\alpha = 25°$.

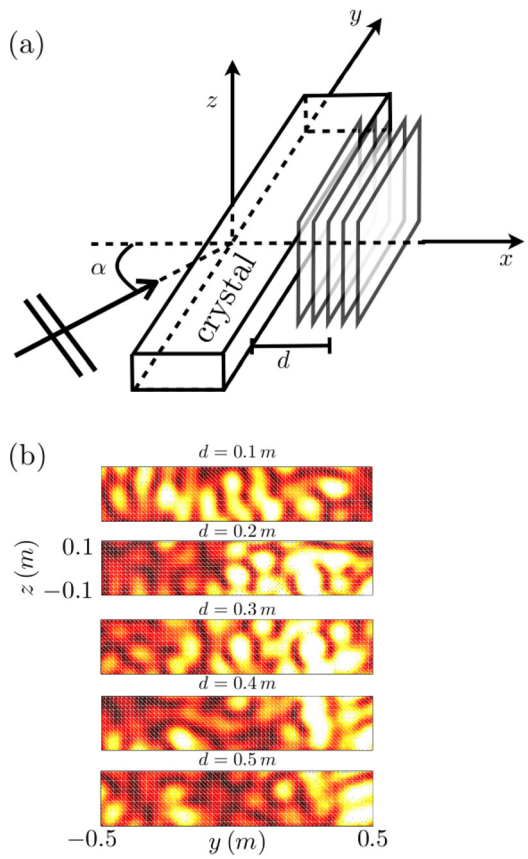

FIG. 9. (Color online) (a) Scheme of the experimental device. (b) Vertical amplitude pressure maps from $d = 0.1$ m (top) to $d = 0.5$ m (low) behind the sonic crystal. The same color scale is used for all the maps.

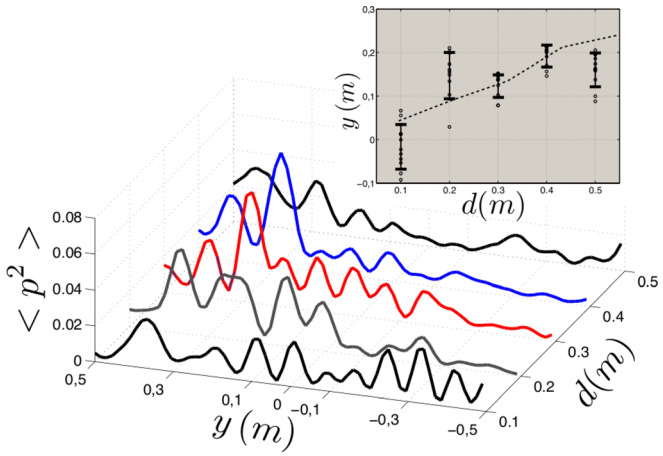

FIG. 10. (Color online) Average value along the z axis of the squared pressure modulus in function of y for $d = [0.1, 0.2, 0.3, 0.4, 0.5]$ m and for $z \in [-0.1 : 0.1]$. The insert shows the positions (○) along the y axis of the weighted mean of $p^2(z)$ for each value of $z \in [-0.1 : 0.1]$ and for $d = [0.1, 0.2, 0.3, 0.4, 0.5]$ m. The vertical lines give the variance of the distribution. The dashed lines shows the position of $\langle p^2(z) \rangle$ estimated with FDTD.

transmitted acoustic beam propagating from the center of the crystal towards a preferential direction in the half-space defined by $y > 0$. We noticed that an acoustic beam for audible frequency range can not be as well defined as in the case of ultrasonic waves. It is remarkable to obtain a transmitted acoustic beam for this frequency range without the self-modulation process. Effectively, the nonlinear effect of the parametric source can not stand at this distance. The beam is not spread inside the SC and the angle of the transmitted beam is approximately α. The negative refraction is noticed because the y coordinate of the transmitted beam center at the exit of the SC is lower than the y coordinate of the incident beam center at the entrance of the SC. If the refraction would have stand in a regular way, the position of the incident center beam would have been located for $y > 0$.

To study the refraction angle of the transmitted beam, the average value of the squared pressure modulus along the z axis for each value of d ($d = [0.1, 0.2, 0.3, 0.4, 0.5]$ m) is performed. The results are shown on the Fig. 10. The negative refraction is clearly highlighted by the distribution of the acoustic intensity along the y axis in function of d: the transmitted beam center is located around $y = 0$ for $d = 0.1$ and moves to $y > 0$ when d is increased. To reinforce this result, the weighted mean of squared pressure modulus p^2 along y for each value of $z \in [-0.1 : 0.1]$ (each horizontal line of the pressure maps in Fig. 9) and for each distance d are presented in the insert of the Fig. 10. The standard deviations σ_d of the distributions are illustrated by the vertical segments with length $2\sigma_d$. The dashed line shows the position of the weighted mean of the squared pressure modulus estimated with a FDTD method performed with the same characteristics as the experimental study (9 rows and 26 lines).

The distribution of the weighted mean of squared pressure modulus is qualitatively in agreement with the attempted result. Due to the nearfield radiations influence, the position of the weighted mean points for the first map (where $d = 0.1$ m is smaller than the wavelength) is underevaluated. In the same way, the position of the weighted mean points for $d = 0.5$ m is also underevaluated because the investigated area is too narrow: one part of the acoustic intensity of the beam is localized to y defined by $y > 0.5$ which allows to an underevaluation of the position. On the contrary, the weighted mean positions for $d = [0.2, 0.3, 0.4]$ m are in agreement with the simulated results. The extended distribution of the weighted mean positions, illustrated by the errorbars on the curve, can be caused by the inherent disorder of the scatterers distribution and also by the error on the incident beam angle. Moreover, the change of impedance between the confined area of the crystal and the free field behind the crystal can explain the relative dispersion of the acoustic beam behind the crystal. But, in spite of these experimental difficulties related to the audible frequency range, this preliminary study points out the existence of negative refraction for acoustic waves in the audible frequency range.

V. CONCLUSION AND PERSPECTIVES

The acoustic band structure of a 2D sonic crystal made up of square cross-section scatterers embedded in air on a square lattice is investigated. The existence of tunable band gaps in the audible frequency range are proved experimentally. This confirms the influence of the scatterer rotation in the unit cell on the band gap width and appearance and demonstrates the efficiency of this type of SC as tunable crystal in the audible frequency range.

Negative refraction is studied through the equifrequency surfaces analysis and FDTD simulation. It is found that such anomalous refraction can happen with scatterer side parallel to the lattice vector, i.e., $\theta = 0°$, for an incident wave of 2300 Hz at $\alpha = 25°$. Negative refraction is demonstrated experimentally by means of 2D vertical maps of the transmitted wave field through the crystal.

A sonic crystal made of square cross-section long rods with an automatic system enabling the control of the angle of rotation of the scatterer is currently under fabrication. This structure will allow us to study more precisely the tunable effect and negative refraction for different angles of rotation of the scatterers experimentally.

ACKNOWLEDGMENTS

The autors wish to thank Bastien Breteau and Miguel Molerón for their help during the experiments and Clément Lagarrigue and Benoit Nenning for their constructive remarks.

[1]E. P. Yablonovitch and T. J. Gmitter, "Photonic band structure: The face centered cubic case," Phys. Rev. Lett. **63**, 1950–1953 (1989).
[2]F. R. Montero de Espinosa, E. Jimenez, and M. Torres, "Ultrasonic band gap in a periodic two-dimensional composite," Phys. Rev. Lett. **80**, 1208–1211 (1998).
[3]V. G. Sanchez-Perez, D. Caballero, R. Martinez-Sala, C. Rubio, J. Sanchez-Dehesa, F. Meseguer, J. Llinares, and F. Galvez, "Sound attenuation by a two-dimensional array of rigid cylinders," Phys. Rev. Lett. **80**, 5325–5328 (1998).
[4]J. O. Vasseur, A. Khelif, P. A. Deymier, Ph. Lambin, B. Djafari-Rouhani, A. Akjouj, L. Dobrzynski, N. Fettouhi, and J. Zemmouri, "Phononic crystal with low filling fraction and absolute acoustic band gap in the audible frequency range: A theoretical and experimental study," Phys. Rev. E **65**, 056608 (2002).

[5]J. O. Vasseur, P. A. Deymier, B. Chenni, B. Djafari-Rouhani, L. Dobrzynski, and D. Prevost, "Experimental and theoretical evidence for the existence of absolute acoustic band gaps in two-dimensional solid phononic crystals," Phys. Rev. Lett **86**, 3012–3015 (2001).
[6]E. Fuster-Garcia, V. Romero-Garcia, J. Sanchez-Perez, and L. Garcia-Raffi, "Targeted band gap creation using mixed sonic crystals arrays including resonators and rigid scatterers," Appl. Phys. Lett. **90**, 244104 (2007).
[7]V. Romero-Garcia, J. Sanchez-Perez, and L. Garcia-Raffi, "Tunable wideband bandstop acoustic filter based on two-dimensional multiphysical phenomena periodic systems," J. Appl. Phys. **110**, 014904 (2009).
[8]D. P. Elford, L. Chalmers, F. V. Kusmartsev, and G. M. Swallowe, "Matryoshka locally resonant sonic crystal," J. Acoust. Soc. Am. **130**, 2746–2755 (2011).
[9]V. Romero-Garcia, J. Sanchez-Perez, L. Garcia-Raffi, J. Herrero, S. Garcia-Nieto, and X. Blasco, "Hole distribution in phononic crystals: Design and optimization," J. Acoust. Soc. Am. **125**, 3774 (2009).
[10]O. Umnova, K. Attenborough, and C. Linton, "Effects of porous covering on sound attenuation by periodic arrays of cylinders," J. Acoust. Soc. Am. **119**, 278–284 (2006).
[11]J. Sanchez-Dehesa, V. M. Garcia-Chocano, D. Torrent, F. Cervera, S. Cabrera, and F. Simon, "Noise control by sonic crystal barriers made of recycled materials," J. Acoust. Soc. Am. **129**, 1173–1183 (2011).
[12]Y. A. Kosevich, C. Goffaux, and J. Sanchez-Dehesa, "Fano-like resonance phenomena by flexural shell modes in sound transmission through two-dimensional periodic arrays of thin-walled hollow cylinders," Phys. Rev. B **74**, 012301 (2006).
[13]A. Krynkin, O. Umnova, A. Y. B. Chong, S. Taherzadeh, and K. Attenborough, "Predictions and measurements of sound transmission through a periodic array of elastic shells in air," J. Acoust. Soc. Am. **128**, 3496–3506 (2010).
[14]C. Goffaux and J. P. Vigneron "Theoretical study of a tunable phononic band gap system," Phys. Rev. B **64**, 075118 (2001).
[15]W. Kuang, Z. Hou, and Y. Liu, "The effects of shapes and symmetries of scatteres on the phononic band gap in 2D phononic crystal," Phys. Rev. Lett. A **332**, 481–490 (2004).
[16]Y. Z. Wang, F. M. Li, and W. H. Wang, "Effects of inclusion shapes on the band gaps in two-dimensional piezoelectric phononic crystals," J. Phys. Condens. Matter **19**, 496204 (2007).
[17]D. Caballero, J. Sanchez-Dehesa, R. Martinez-Sala, J. V. Sanchez-Perez, F. Meseguer, and J. Llinares, "Large two-dimensional sonic band gaps," Phys. Rev. E **60**, R6316–R6319 (1999).
[18]C. Goffaux, F. Maseri, J. O. Vasseur, B. Djafari-Rouhani, and Ph. Lambin, "Measurements and calculations of the sound attenuation by a phononic band gap structure suitable for an insulating partition application," Appl. Phys. Lett. **83**, 281–284 (2003).
[19]V. Veselago, "The electrodynamics of substances with simultaneously negative values of ϵ and μ," Sov. Phys. Usp. **10**, 510–514 (1968).
[20]J. B. Pendry, "Extremely low frequency plasmons in metallic microstructures," Phys. Rev. Lett. **76**, 4773–4785 (1996).
[21]J. B. Pendry, A. J. Holden, D. J. Robbins, and W. J. Stewart, "Low frequency plasmons in thin-wire structures," J. Phys. Condens. Matter **10**, 4785 (1998).
[22]M. Notomi, "Theory of light propagation in strongly modulated photonic crystals: Refractionlike behavior in the vicinity of the photonic band gap," Phys. Rev. B **62**, 10696–10705 (2000).
[23]C. Luo, S. G. Johnson, J. D. Joannopoulos, and J. B. Pendry, "Subwavelength imaging in photonic crystals," Phys. Rev. B **68**, 045115 (2003).
[24]X. Hu, Y. Shen, X. Liu, R. Fu, and J. Zi, "Complete band gaps for liquid surface waves propagating over a periodically drilled bottom," Phys. Rev. E **68**, 066308 (2003).
[25]X. Hu, Y. Shen, X. Liu, R. Fu, and J. Zi, "Superlensing effect in liquid surface waves," Phys. Rev. E **69**, 030201 (2004).
[26]A. Sukhovich, L. Jing, and J. H. Page, "Negative refraction and focusing of ultrasound in two-dimensional phononic crystals," Phys. Rev. B **77**, 014301 (2008).
[27]S. Zhang, L. Yin, and N. Fang, "Focusing ultrasound with an acoustic metamaterial network," Phys. Rev. Lett. **102**, 194301 (2009).
[28]C. Croenne, E. Manga, B. Morvan, A. Tinel, B. Dubus, J. Vasseur, and A. Hladky-Hennion, "Negative refraction of longitudinal waves in a two-dimensional solid-solid phononic crystal," Phys. Rev. B **83**, 054301 (2011).
[29]A. Hladky-Hennion, C. Croenne, B. Dubus, J. Vasseur, L. Haumesser, D. Manga, and B. Morvan, "Negative refraction of elastic waves in a 2D phononic crystal: Contribution of resonant transmissions to the construction of the image of a point source," AIP Adv. **1**, 041405 (2011).
[30]B. Morvan, A. Tinel, A. Hladky-Hennion, J. Vasseur, and B. Dubus, "Experimental demonstration of the negative refraction of a transverse elastic wave in a two-dimensional solid phononic crystal," Appl. Phys. Lett. **96**, 101905 (2010).
[31]B. Bonello, L. Belliard, J. Pierre, J. O. Vasseur, B. Perrin, and O. Boyko, "Negative refraction of surface acoustic waves in the subgigahertz range," Phys. Rev. B **82**, 104109 (2010).
[32]S. Feng, Z.-Y. Li, Z.-F. Feng, K. Ren, B.-Y. Cheng, and D.-Z. Zhang, "Focusing properties of a rectangular-rod photonic-crystal slab," J. Appl. Phys. **98**, 063102 (2005).
[33]Y. Huang, W. Lu, and S. Sridhar, "Alternative approach to all-angle negative refraction in two-dimensional photonic crystals," Phys. Rev. B **76**, 013824 (2007).
[34]L. Feng, X.-P. Liu, M.-H. Lu, Y.-B. Chen, Y.-F. Chen, Y.-W. Mao, J. Zi, Y.-Y. Zhu, S.-N. Zhu, and N.-B. Ming, "Refraction control of acoustic waves in a square-rod-constructed tunable sonic crystal," Phys. Rev. B **73**, 193101 (2006).
[35]J. Bucay, E. Roussel, J. O. Vasseur, P. A. deymier, A.-C. Hladky-Hennion, Y. Pennec, K. Muralidharan, B. Djafari-Rouhani, and B. Dubus, "Positive, negative, zero refraction and beam splitting in a solid/air phononic crystal: Theoretical end experimental study," Phys. Rev. B **79**, 214305 (2009).
[36]A. Duclos, D. Lafarge, and V. Pagneux, "Transmission of acoustics waves through 2D phononic crystal: Visco-thermal and multiple scattering effect," Eur. Phys. J. **45**, 319–324 (2009).
[37]X. Li, F. Wu, H. Hu, S. Zhong, and Y. Liu, "Large acoustic band gaps created by rotating square rods in two-dimensional periodic composites," J. Phys. D: Appl. Phys. **36**, 15 (2003).
[38]F. Wu, Z. Liu, and Y. Liu, "Acoustic band gaps created by rotating square rods in two-dimensional lattice," Phys. Rev. E **66**, 046628 (2002).
[39]F. J. Pompei, "The use of airbone ultrasonics for generating audible sound beams," J. Audio Eng. Soc. **47**, 726–731 (1999).
[40]M. S. Kushwaha, P. Halevi, L. Dobrzynski, and B. Djafari-Rouhani, "Acoustic band structure of periodic elastic composites," Phys. Rev. Lett. **71**, 2022–2025 (1993).
[41]C. Luo, S. Jonhson, J. Joannopoulos, and J. Pendry, "All-angle negative refraction without negative effective index," Phys. Rev. B **65**, 201104 (2002).
[42]J. Redondo, R. Pico, and B. Roig, "Time domain simulation of sound diffusers using finite-difference schemes" Acta Acust. Acust. **93**, 611–622 (2007).